Transition State P-glycoprotein Binds Drugs and Modulators with Unchanged Affinity, Suggesting a Concerted Transport Mechanism†

Qin Qu, Joseph W. K. Chu, and Frances J. Sharom*

Department of Chemistry and Biochemistry, University of Guelph, Guelph, Ontario, Canada N1G 2W1

Received September 3, 2002; Revised Manuscript Received November 28, 2002

ABSTRACT: The P-glycoprotein multidrug transporter is a plasma membrane efflux pump for hydrophobic natural products, drugs, and peptides, driven by ATP hydrolysis. Determination of the details of the catalytic cycle of P-glycoprotein is critical if we are to understand the mechanism of drug transport and design ways to inhibit it. It has been proposed that the vanadate-trapped transition state of P-glycoprotein (Pgp·ADP·V_i·M^{2+}, where M^{2+} is a divalent metal ion) has a very low affinity for drugs compared to resting state protein, thus leading to binding of substrate on the cytoplasmic side of the membrane and release of substrate to the extracellular medium (or the extracellular membrane leaflet). We have used several different fluorescence spectroscopic approaches to show that isolated purified P-glycoprotein, when trapped in a stable transition state with vanadate and either Co^{2+}or Mg^{2+}, binds drugs with high affinity. For vinblastine, colchicine, rhodamine 123, and doxorubicin, the affinity of the vanadate-trapped transition state for drugs was only very slightly (less than 2-fold) lower than the binding affinity of resting state Pgp, whereas for the modulators cyclosporin A and verapamil and the substrate Hoechst 33342, the binding affinity was very similar for the two states. The drug binding affinity of the ADP-bound form of the transporter was also comparable to that of the unoccupied transporter. These results suggest that release of drug from the transporter during the catalytic cycle precedes formation of the transition state.

The ABC[1] superfamily represents one of the largest and most important families of membrane proteins in both prokaryotes and eukaryotes (*1*−*4*). ABC proteins carry out either import or export of their substrates across the plasma membrane or organelle membranes of cells (*5*), powered by ATP hydrolysis at two cytosolic nucleotide binding (NB) domains (*6*, *7*). The multidrug transporters represent a very important subset of the ABC superfamily, since they are responsible for resistance to antibiotics and antifungal agents in microorganisms (*8*−*11*) and resistance to multiple chemotherapeutic agents in many human cancers (*12*−*14*). Defective ABC transporters have also been implicated in a number of human diseases (*15*). Understanding the catalytic cycle of ABC transporters is thus an important goal and is necessary if we are to develop strategies for modulating the function of this group of proteins.

The most studied ABC multidrug transporter is the MDR1 P-glycoprotein (Pgp), which acts as an efflux pump for hundreds of hydrophobic natural products, drugs, and peptides of diverse structure (*16*, *17*). The protein has been proposed to behave as a "hydrophobic vacuum cleaner", removing toxic compounds from the membrane to the extracellular medium (*18*). The drug binding sites of Pgp are likely accessible from the lipid bilayer, rather than the aqueous phase, and the partitioning of the transport substrate into the membrane plays an important role in modulating both drug binding to the protein (*19*) and the rate of drug transport (*20*). Recent work in our laboratory using fluorescence resonance energy transfer (FRET) has localized the binding site for the drug substrate Hoechst 33342 to the cytoplasmic leaflet of the bilayer (*21*). This is in keeping with the proposal that Pgp may be a drug flippase (*18*), moving its substrates from the cytoplasmic leaflet to the extracellular leaflet of the membrane, and indeed, reconstituted Pgp can flip a variety of fluorescently labeled phospholipids from one leaflet of the bilayer to the other (*22*).

Considerable progress has been made in the past few years toward understanding both the structure and the catalytic cycle of Pgp. Two recent structures of complete bacterial ABC transporters, the lipid flippase MsbA (*23*) and the vitamin B_{12} importer BtuCD (*24*), showed different modes of interaction for the two NB domains. In the MsbA structure, the two domains were quite widely separated and not in direct contact, whereas they were closely interdigitated in BtuCD. The latter structure resembled that previously modeled by Jones and George (*25*) and later reported for Rad50cd (*26*), where each domain contributes residues to the active site of the partner domain. Biochemical evidence that the NB subunits of the bacterial maltose permease are also arranged in this fashion was recently reported (*27*). Likewise, the NB domains of Pgp appear to be closely associated (*28*, *29*), similar to the organization of Rad50cd and BtuCD.

† This work was supported by a grant to F.J.S. from the National Cancer Institute of Canada, with funds provided by the Canadian Cancer Society.

* Correspondence should be addressed to this author. Phone: 519-824-4120 ext 2247. Fax: 519-766-1499. E-mail: fsharom@uoguelph.ca.

[1] Abbreviations: ABC, ATP binding cassette; CHAPS, 3-[(3-cholamidopropyl)dimethylammonio]-1-propanesulfonate; FRET, fluorescence resonance energy transfer; H33342, Hoechst 33342; IAAP, iodoarylazidoprazosine; MDR, multidrug resistance/resistant; MIANS, 2-(4′-maleimidylanilino)naphthalene-6-sulfonic acid; NB, nucleotide binding; Pgp, P-glycoprotein.

10.1021/bi0267745 CCC: $25.00
Published on Web 01/17/2003

Studies with vanadate trapping have led to considerable insight into the catalytic cycle of Pgp. Following ATP hydrolysis and the dissociation of P_i, orthovanadate can enter the active site of one NB domain and form a stable pentacoordinate complex consisting of Pgp·ADP·V_i·M^{2+}, where M^{2+} is a divalent cation (Mg^{2+}, Mn^{2+}, or Co^{2+}) (*30*). The vanadate-trapped state is thought to mimic the catalytic transition state of the protein during the normal ATP hydrolysis pathway. Vanadate trapping results in abolition of ATPase activity at both NB domains, leading to the proposal that the two active sites of Pgp cooperate during catalysis and alternately carry out ATP hydrolysis (*31*). Slow loss of vanadate from the active site leads to restoration of ATPase activity, with the rate of recovery depending on the divalent cation (*30*).

The vanadate-trapped transition state represents a very useful tool for dissecting the catalytic cycle of Pgp. The conformation of the transition state appears to be significantly different from that of the resting state of the protein, as shown by proteolysis (*32*) and electron microscopy studies (*33*). It has been reported that vanadate-trapped Pgp shows greatly reduced photoaffinity labeling by the substrate analogue [^{125}I]iodoarylazidoprazosine (IAAP) (*34*), and on the basis of these results, it was proposed that the transition state has a much lower [30-fold (*35*)] binding affinity for drugs. A mechanism was proposed whereby a change in the "sidedness" of the drug binding site, together with a large drop in binding affinity, would lead to release of transport substrate from the transition state complex to the extracellular side (or the extracellular leaflet) of the membrane. On the basis of trypsin susceptibility experiments, Zhang and co-workers proposed that the ADP-bound form of Pgp also has very low affinity for binding the MDR drug vinblastine (*36*).

In the present work, we prepared purified transition state Pgp by trapping of ADP·V_i in one active site, using both Co^{2+} and Mg^{2+}, to form a stable complex. Several different fluorescence spectroscopic approaches were then used to quantitate the binding of drugs and modulators to transition state Pgp and to ADP-bound protein. We found that both vanadate-trapped Pgp and ADP-bound Pgp showed essentially unchanged drug binding affinity compared to resting state protein. These results imply that release of drug from the transporter during the catalytic cycle precedes the formation of the transition state and provide evidence that drug transport takes place via a concerted mechanism.

MATERIALS AND METHODS

Materials. 3-[(3-Cholamidopropyl)dimethylammonio]-1-propanesulfonate (CHAPS), Na_2ATP, sodium orthovanadate, vinblastine, colchicine, rhodamine 123, doxorubicin, and verapamil were obtained from Sigma Chemical Co. (St. Louis, MO). Cyclosporin A was provided by Pfizer Central Research (Groton, CT). 2-(4′-maleimidylanilino)naphthalene-6-sulfonic acid (MIANS) and Hoechst 33342 (H33342) were supplied by Molecular Probes (Eugene, OR).

Purification of Pgp. Pgp was purified from plasma membrane vesicles isolated from the MDR Chinese hamster ovary cell line CH^RB30, as previously described (*21*, *28*). Plasma membrane vesicles were stored frozen at −70 °C for no longer than 3 months before use. The purified protein (90−95%) was obtained in 2 mM CHAPS in 50 mM Tris-HCl/0.15 M NaCl/5 mM $MgCl_2$, pH 7.5, stored on ice, and used within 24 h. The protein concentration of purified Pgp was determined as described by Peterson (*37*) using bovine serum albumin (crystallized and lyophilized, Sigma) as a standard.

Preparation of Vanadate-Trapped Transition State Pgp. A stock solution of 100 mM sodium orthovanadate was prepared at pH 10, and aliquots were boiled for 4 min before use to degrade polymeric species. For preparation of the Co^{2+} form of transition state Pgp, a 300 μg aliquot of purified protein was incubated at 37 °C in a total volume of 1.5 mL of CHAPS buffer (2 mM CHAPS/50 mM Tris-HCl/0.15 M NaCl, pH 7.5) in the presence of 5 mM $CoCl_2$, 1 mM ATP, and 0.2 mM vanadate. After 20 min, the mixture was eluted through a Bio-Gel P6 gel filtration column (Bio-Rad Laboratories, Mississauga, Ontario, Canada) preequilibrated with 2 mM CHAPS buffer to remove excess ATP, vanadate, $CoCl_2$, and P_i, and transition state Pgp was collected. The Mg^{2+} form of the transition state complex was prepared by incubating 300 μg of Pgp at 37 °C in a total volume of 1.5 mL of CHAPS buffer (2 mM CHAPS/50 mM Tris-HCl/0.15 M NaCl, pH 7.5) in the presence of 5 mM $MgCl_2$, 1 mM ATP, and 0.2 mM vanadate. In this case, because of the shorter lifetime of the Mg^{2+} complex, the excess reagents were not removed, so that any reactivated complex would be immediately reconverted to the trapped state. The Mg^{2+}-dependent ATPase activity of the Pgp transition state complexes was determined both before and immediately after the spectroscopic measurements by measuring the release of P_i using a colorimetric method (*38*, *39*). ATPase assays were carried out for 5 min at 37 °C in assay buffer (50 mM Tris-HCl/0.15 M NaCl/5 mM $MgCl_2$, pH 7.5) in the presence of 1 mM ATP. Both the Co^{2+} transition state complex and the Mg^{2+} transition state complex showed insignificant ATPase activity at both time points.

Labeling of Resting State and Transition State Pgp with MIANS. For measurement of drug affinity to resting state Pgp by MIANS quenching, Pgp was labeled with MIANS at both NB domains (*40*). Purified Pgp (∼200 μg) in a total volume of 1 mL in 2 mM CHAPS/50 mM Tris-HCl, pH 7.5, was incubated with 30 μM MIANS at 22 °C for 30 min in the dark. Protein labeled with MIANS at both NB domains (Pgp-2MIANS) was separated from unreacted MIANS by passing through a Bio-Gel P-6 gel filtration column equilibrated with 2 mM CHAPS buffer. To prepare transition state Pgp labeled with MIANS at only one NB domain (Pgp-V_i-MIANS), Co^{2+}-trapped Pgp prepared as described above was incubated with 30 μM MIANS at 22 °C for 30 min in the dark. To remove unreacted MIANS, the sample was passed through a Bio-Gel P6 gel filtration column preequilibrated with 2 mM CHAPS buffer. Samples of Pgp-2MIANS and Pgp-V_i-MIANS were adjusted to the same protein concentration of 50 μg/mL.

Fluorescence Measurements. Fluorescence spectra were recorded on a PTI Alphascan-2 spectrofluorometer (Photon Technology International, London, Ontario, Canada) with the cell holder thermostated at 22 °C and a 2 nm excitation and emission band-pass. A built-in automatic correction system was used to correct the emission spectra of labeled Pgps. Studies of fluorescence quenching of MIANS-labeled resting state and transition state Pgp by various substrates were

carried out in the presence of large unilamellar vesicles of asolectin (soybean phospholipids). Large unilamellar asolectin vesicles were prepared by extrusion through 100 nm polycarbonate filters (*41*, *42*) and added to the Pgp solution at the final concentration of 0.5 mg/mL. The working solutions of drugs and modulators were also prepared in 2 mM CHAPS containing 0.5 mg/mL asolectin. Controls containing unlabeled Pgp were used to correct the measured fluorescence intensity for light scattering. The inner filter effect was corrected at both the excitation and emission wavelengths as described previously (*40*, *43*, *44*), using the equation:

$$F_{\mathrm{icor}} = (F_{\mathrm{i}} - B)(V_i/V_0) \times 10^{0.5b(A_{\lambda\mathrm{ex}}+A_{\lambda\mathrm{em}})}$$

where F_{icor} is the corrected value of the fluorescence intensity, F_{i} is the experimentally measured fluorescence intensity, B is the background fluorescence intensity caused by scattering, V_0 is the initial volume of the sample, V_i is the volume of the sample at a given point in the titration, b is the path length of the optical cell in centimeters, and $A_{\lambda\mathrm{ex}}$ and $A_{\lambda\mathrm{em}}$ are the absorbance of the sample at the excitation and emission wavelengths, respectively.

Determination of the Affinity of Drug Binding to Resting and Transition State Pgp Using MIANS Quenching. A fixed concentration of MIANS-labeled resting state Pgp (Pgp-2MIANS) or MIANS-labeled transition state Pgp (Pgp-V_i-MIANS) was titrated at 22 °C with increasing concentrations of drugs and modulators. Fluorescence quenching titrations were performed by successively adding 5 μL aliquots of drug working solution to 500 μL of MIANS-labeled Pgp, in the presence or absence of 3 mM ADP. The steady-state MIANS fluorescence was measured at 420 nm for 20 s at an excitation wavelength of 322 nm. Quenching of MIANS fluorescence at various drug concentrations was fitted to the following equation, which describes binding to a single affinity site:

$$\Delta F/F_0 \times 100 = \frac{(\Delta F_{\mathrm{max}}/F_0 \times 100)[\mathrm{S}]}{K_{\mathrm{d}} + [\mathrm{S}]}$$

where $(\Delta F/F_0 \times 100)$ represents the percent change in fluorescence intensity relative to the initial value after addition of drug at a concentration [S], $(\Delta F_{\mathrm{max}}/F_0 \times 100)$ is the maximum percent quenching of the fluorescence intensity that occurs upon saturation of the drug binding site, and K_{d} is the dissociation constant for binding of drug to Pgp. Experimental quenching data were fitted to the binding equation by regression analysis using SigmaPlot, and the value of K_{d} was extracted.

Determination of the Affinity of Drug Binding to Resting and Transition State Pgp Using Intrinsic Trp Quenching. Drug binding to Pgp was also quantitated using quenching of the intrinsic Trp fluorescence of the protein by bound drug, as previously described (*45*). A fixed concentration of Pgp in either the resting state or the Mg^{2+}-trapped transition state (prepared as described above) was titrated with increasing concentrations of drug or modulator. The Trp residues of Pgp were excited at 295 nm, and after each addition of substrate, the steady-state fluorescence intensity was recorded at 325 nm. The fluorescence intensities were corrected for dilution, scattering, and the inner filter effect as described above. The experimental Trp quenching data were fitted to an equation for binding to a single site (see above), and the value of K_{d} was determined.

Determination of the Affinity of Drug Binding to Resting and Transition State Pgp Using Enhancement of H33342 Fluorescence. Binding of H33342 to Pgp was quantitated using enhancement of H33342 fluorescence upon binding to Pgp, as previously described (*21*). A fixed concentration of Pgp in either the resting state or the Mg^{2+}-trapped transition state (prepared as described above) was titrated with increasing concentrations of H33342. The fluorescence emission of the drug was determined at 460 nm following excitation at 350 nm. The following equation was used to correct the fluorescence enhancement data:

$$F_{\mathrm{icor}} = (F_{\mathrm{i}} - B_{\mathrm{i}})(V_i/V_0) \times 10^{0.5b(A_{\lambda\mathrm{em}}+A_{\lambda\mathrm{em}})}$$

where B_{i} is the fluorescence intensity of free H33342 in 2 mM CHAPS buffer. The H33342 fluorescence enhancement data were fitted to the equation:

$$\Delta F = \Delta F_{\mathrm{max}}[\mathrm{S}]/(K_{\mathrm{d}} + [\mathrm{S}])$$

where ΔF represents the increase in fluorescence intensity relative to the initial value after addition of H33342 at a concentration [S], and ΔF_{max} is the maximum enhancement in fluorescence intensity that occurs upon saturation of the drug binding site, and a value for K_{d} was estimated.

Photoaffinity Labeling of Resting and Transition State Pgp with [^{3}H]Azidopine. Co^{2+}-trapped transition state Pgp was prepared as described above. Photoaffinity labeling was carried out according to Loe and Sharom (*46*). Briefly, purified resting state or transition state Pgp (~2.5 μg) was incubated at room temperature (22 °C) or on ice in 50 mM Tris-HCl/0.15 M NaCl, pH 7.4, with [^{3}H]azidopine (200 nM, 51 Ci/mmol; Amersham Biosciences) in the presence or absence of 1 mM ATP, 200 μM orthovanadate, and 5 mM Mg^{2+} for 20 min under subdued light. The samples were then illuminated with a UV lamp for 20 min either at room temperature or on ice. Samples were analyzed by SDS−PAGE on a 10% Tris−glycine gel, followed by autoradiography. The Pgp band intensities on the autoradiograms were quantitated by scanning densitometry, followed by analysis using Scion Imaging software (Scion Corp., Frederick, MD).

RESULTS

Transition State Pgp. Transition state Pgp was prepared by trapping either ADP·V_i·Co^{2+} or ADP·V_i·Mg^{2+} in one of the NB domain active sites. We and others have previously shown that trapping of vanadate in one of the catalytic sites using Co^{2+} as the divalent cation produces a highly stable transition state complex (*21*, *30*). The Co^{2+} complex loses V_i and ADP from the active site, with recovery of ATPase activity, quite slowly compared to the situation when Mg^{2+} is used. Only ~10% activity is regained after 3 h (*21*), allowing MIANS labeling and subsequent spectroscopic experiments to be carried out. In the case of the stable Co^{2+}-trapped complex, excess reagents (ATP, $CoCl_2$, V_i, P_i, etc.) were removed by gel filtration chromatography prior to carrying out fluorescence experiments. ATPase activity

measurements were carried out both before and after the spectroscopic analysis to confirm that the inactive transition state had been achieved and that no significant amounts of active Pgp had been re-formed during this time period.

Experiments were also conducted with the Mg^{2+} form of the vanadate-trapped transition state. In this case, the complex is less stable and loses V_i and ADP more rapidly when excess reagents are removed (half-time of ~60 min at 37 °C) (*28*, *30*), reverting to catalytically active resting state Pgp. In this case, to prevent exit from the transition state during the spectroscopic experiments, excess ATP, $MgCl_2$, and V_i were not removed, so that any resting state Pgp is immediately converted back into the transition state complex. ATPase activity measurements confirmed that the transition state complex was formed and was still present at the completion of the spectroscopic experiments.

Affinity of Drug Binding to MIANS-Labeled Resting State and Transition State Pgp Using Quenching of MIANS Fluorescence. Purified Pgp is labeled with the sulfhydryl-reactive fluorophore MIANS via covalent modification of Cys 428 and Cys 1071 (*40*, *47*) within the Walker A motifs of the NB domains (Pgp-2MIANS). Photoaffinity labeling and fluorescence studies have shown that MIANS-labeled Pgp binds drugs and nucleotides with normal affinity (*40*, *48*, *49*). Its ATPase activity is inactivated likely by a steric effect. The protein can be loaded with drug and ATP but will not progress further, which is an advantage when dissecting out the conformational changes associated with the catalytic cycle. We previously showed that MIANS-labeled Pgp was quenched in a saturable, concentration-dependent fashion by MDR drugs and modulators and that this property could be used to quantitate dissociation constants for binding of these compounds to the transporter (*40*). MIANS quenching was attributed to a conformational change in the protein following interaction of the drug with the putative membrane-embedded substrate binding site, which alters the local environment of the MIANS probe in the NB domains. This "cross-talk" between domains of the protein is presumably part of the mechanism by which ATP hydrolysis is coupled to drug binding to power transport. In the present study, both untreated resting state Pgp and the Co^{2+}-trapped transition state Pgp were labeled with MIANS at the Cys residues in the Walker A motifs of the NB domains. In the case of resting state Pgp, two MIANS groups are incorporated, one in each active site (*40*), giving Pgp-2MIANS, whereas for vanadate-trapped Pgp, only the Cys in the unoccupied active site is labeled, producing Pgp-V_i-MIANS (*28*).

Addition of various drugs and modulators was carried out using three purified Pgp samples in parallel: the resting state in the absence of added nucleotide (NB domains unoccupied), the resting state with added ADP (ADP bound), and the Co^{2+} transition state complex (NB domains unoccupied). As shown in Figure 1, the MDR transport substrates vinblastine and doxorubicin produced saturable quenching of the MIANS label in the Co^{2+} transition state complex, as well as the resting state protein with both unoccupied NB domains and with ADP bound. All three quench curves were quite similar in terms of overall appearance and the maximum level of quenching reached. Estimation of the K_d values for binding by curve fitting indicated that nucleotide-free and ADP-bound resting state Pgp has very similar

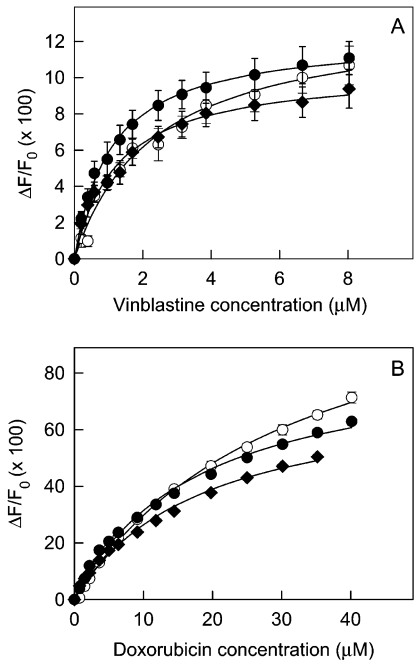

FIGURE 1: Quenching of MIANS-labeled Pgp fluorescence on binding of the MDR drugs, vinblastine (A) and doxorubicin (B). Solutions (200 μg/mL) of untreated resting state Pgp (Pgp-2MIANS, ●), the Co^{2+} form of vanadate-trapped Pgp (Pgp-V_i-MIANS, ○), and ADP-bound Pgp-2MIANS (◆) were titrated with drug at 22 °C, and the fluorescence emission at 420 nm was recorded after excitation at 322 nm. The quenching data were fitted to a binding equation (solid line), and a value for K_d was estimated. The same batch of Pgp was used for resting state, ADP-bound, and transition state experiments. Titrations were carried out in duplicate. Where error bars are not visible, they are contained within the symbols.

Table 1: Binding Affinity of Resting State and Transition State Pgp for Drugs and Modulators Determined Using MIANS Quenching[a]

	K_d (μM)[a]		
drug	resting state Pgp-2MIANS	transition state Pgp-V_i-MIANS	resting state ADP-bound Pgp-2MIANS
MDR drugs			
vinblastine	1.08 ± 0.06	2.32 ± 0.32	1.27 ± 0.13
rhodamine 123	17.5 ± 0.8	24.2 ± 0.1	18.7 ± 0.9
doxorubicin	17.9 ± 1.4	32.1 ± 1.9	18.2 ± 1.8
colchicine	111 ± 12	188 ± 24	138 ± 19
modulators			
verapamil	2.97 ± 0.16	3.10 ± 0.19	3.26 ± 0.17
cyclosporin A	0.517 ± 0.047	0.491 ± 0.034	0.603 ± 0.025

[a] Three independent experiments were carried out for determination of each value of K_d, with different preparations of Pgp and Pgp-V_i-MIANS in each case. Means ± SEM are indicated.

affinities for binding vinblastine and doxorubicin (see Table 1). The Co^{2+} transition state complex, on the other hand, had a slightly (~2-fold) lower drug binding affinity. Similar results were noted for two other structurally unrelated MDR drugs, rhodamine 123 and colchicine. The transition state complex was found to have a slightly higher K_d value compared to the resting state protein, whether it was free of nucleotide or ADP bound (Table 1).

Figure 2 shows the results observed following addition to the various MIANS-labeled Pgp complexes of two commonly used MDR modulators, verapamil and cyclosporin A. Once again, very similar quench curves were noted. In both cases, the Co^{2+} transition state complex and ADP-bound

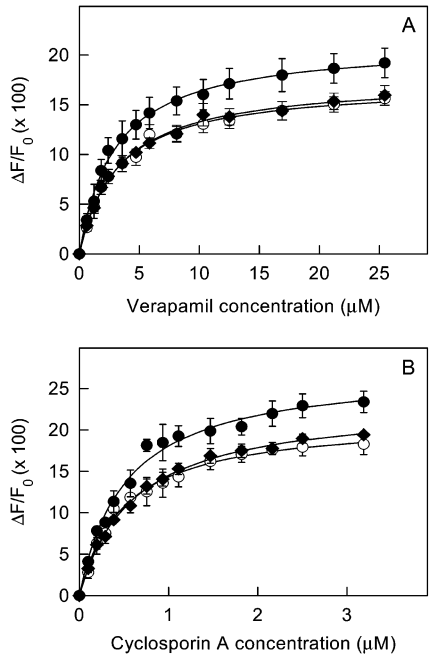

FIGURE 2: Quenching of MIANS-labeled Pgp fluorescence on binding of the MDR modulators, verapamil (A) and cyclosporin A (B). Solutions (200 μg/mL) of untreated resting state Pgp (Pgp-2MIANS, ●), the Co^{2+} form of vanadate-trapped Pgp (Pgp-V_i-MIANS, ○), and ADP-bound Pgp-2MIANS (◆) were titrated with modulator at 22 °C, and the fluorescence emission at 420 nm was recorded after excitation at 322 nm. The quenching data were fitted to a binding equation (solid line), and a value for K_d was estimated. The same batch of Pgp was used for resting state, ADP-bound, and transition state experiments. Titrations were carried out in duplicate. Where error bars are not visible, they are contained within the symbols.

resting state protein showed slightly lower levels of maximum quenching compared to nucleotide-free resting state Pgp. Determination of binding affinity showed that all three forms of Pgp had very similar K_d values (Table 1), with the ADP-bound complex showing a tendency to a very slightly lower affinity. Thus it appears as if both the transition state and ADP-bound forms of MIANS-labeled Pgp can bind a variety of drugs and modulators with the same affinity as resting state protein.

Using binding of [^{3}H]vinblastine to Pgp by a filtration method, Callaghan and co-workers reported that Pgp has a 10-fold higher affinity binding site (K_d = 80 nM) in addition to a site of similar affinity to that found here (0.7 μM) (*50*). To date, there have been no other reports of a very high affinity binding site for vinblastine. The vinblastine binding affinity found by the fluorescence experiments in this work is very similar to that reported by Druley et al. using antibody binding (*51*) and Doppenschmitt et al. (*52*), who employed a radioligand binding assay.

Affinity of Drug Binding to Resting State and Transition State Pgp Using Quenching of Intrinsic Trp Fluorescence. We now wished to test whether native unmodified Pgp can bind drugs when in the transition state and the ADP-bound form. Binding of drugs and modulators to purified Pgp results in quenching of the intrinsic Trp fluorescence of the native protein (*45*). We previously showed that this quenching likely results from FRET between membrane-bound Trp residues and the drug molecule. Trp quenching is saturable and concentration dependent, so that fitting of the experimental

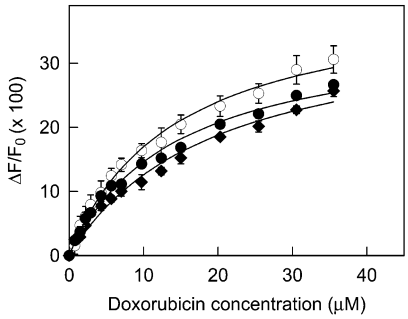

FIGURE 3: Quenching of Pgp intrinsic Trp fluorescence on binding of doxorubicin. Solutions (100 μg/mL) of untreated resting state Pgp (●), the Mg^{2+} form of vanadate-trapped Pgp (○), and ADP-bound Pgp (◆) were titrated with drug at 22 °C, and the fluorescence emission at 325 nm was recorded after excitation at 295 nm. The quenching data were fitted to a binding equation (solid line), and a value for K_d was estimated. The same batch of Pgp was used for resting state, ADP-bound, and transition state experiments. Titrations were carried out in duplicate. Where error bars are not visible, they are contained within the symbols.

Table 2: Drug Binding Affinity of Resting State and Transition State Pgp Determined Using Trp Quenching[a]

	K_d (μM)		
drug	resting state	transition state	resting state ADP bound
vinblastine	1.62 ± 0.16	2.06 ± 0.37	1.66 ± 0.26
doxorubicin	14.4 ± 1.56	14.2 ± 1.29	19.4 ± 2.90

[a] Three independent experiments were carried out for determination of each value of K_d, with different preparations of Pgp in each case. Means ± SEM are indicated.

data to a binding equation can be used to estimate K_d values for drug binding (*45*). In these experiments, we used the Mg^{2+} form of the transition state complex in the presence of excess reagents to prevent exit from the transition state. Titration of the three forms of Pgp with doxorubicin led to saturable quenching of the Trp fluorescence (Figure 3). The transition state complex showed a somewhat higher maximum quenching, but overall the three curves were comparable and the estimated K_d values were also in the same range (Table 2). Similar results were obtained for vinblastine (Table 2). Thus, the native (unmodified) Mg^{2+}-trapped transition state complex is also able to bind MDR drugs with normal affinity, as is the ADP-bound form of the protein.

Affinity of Hoechst 33342 Binding to Resting State and Transition State Pgp Using Enhancement of Fluorescence. The lipophilic dye, H33342, is known to be transported by both plasma membrane-bound Pgp (*53*) and purified Pgp (*54*). More recently, we showed that H33342 bound to Pgp with high affinity (K_d = ~1−2 μM) and that direct interaction of the drug with the hydrophobic substrate binding site of the purified transporter led to a large enhancement of its fluorescence emission (*21*). As shown in Figure 4, titration of H33342 with resting state Pgp led to a concentration-dependent, saturable increase in the fluorescence emission of the dye. A K_d value of 1.22 μM was estimated by fitting of the experimental data to an equation for a single affinity binding site (see Materials and Methods). The Mg^{2+} form of vanadate-trapped Pgp also showed saturable fluorescence enhancement, indicating that the transition state complex is still able to bind this drug (Figure 4). The binding affinity of vanadate-trapped Pgp was almost identical to

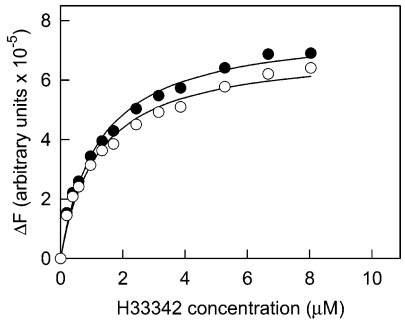

FIGURE 4: Enhancement of H33342 fluorescence on binding to resting state and transition state Pgp. Solutions (70 μg/mL of protein) of untreated resting state Pgp (●) and the Mg^{2+} form of vanadate-trapped Pgp (○) were titrated with increasing concentrations of H33342 at 22 °C. The enhanced fluorescence emission of the dye at 460 nm was measured following excitation at 350 nm. The enhancement data were fitted to a binding equation (solid line), and a value for K_d was estimated. The same batch of Pgp was used for resting state and transition state experiments. Where error bars are not visible, they are contained within the symbols.

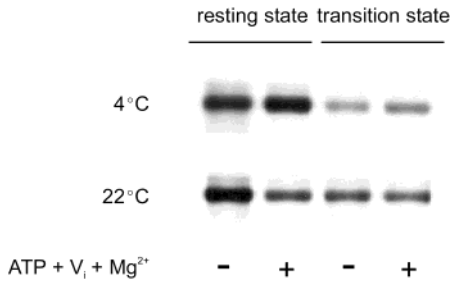

FIGURE 5: Photoaffinity labeling of resting state and vanadate-trapped transition state Pgp with azidopine at 4 and 22 °C. Purified Pgp (2.5 μg), either untreated or after trapping with vanadate and Co^{2+}, was incubated at either 22 °C or on ice with 200 nM [^{3}H]azidopine. After a 20 min incubation in the absence or presence of 1 mM ATP, 200 μM vanadate, and 5 mM $MgCl_2$, the samples were cross-linked by UV exposure for 20 min, either at 22 °C or on ice. The samples were then analyzed by SDS−PAGE and autoradiography. The intensities of the Pgp bands on the autoradiograms were quantitated by scanning densitometry, followed by image analysis.

that of the resting state protein, with an estimated K_d of 1.20 μM.

Photoaffinity Labeling of Resting State and Transition State Pgp with Azidopine. We wished to determine whether the reduction in IAAP photolabeling reported for transition state Pgp (*34*) could also be observed for the substrate analogue azidopine. We have previously shown that both Pgp and Pgp-2MIANS can be photolabeled with [^{3}H]azidopine and that this labeling is subject to competition by vinblastine and other substrates (*49*, *55*, *56*). Photolabeling experiments were carried out with purified resting state Pgp and the Co^{2+} form of the vanadate-trapped transition state, with all excess reagents removed, at two temperatures, either 22 °C or 4 °C. Previously reported studies did not remove excess reagents before UV cross-linking, so to simulate this situation, samples were incubated either alone or in the presence of added 1 mM ATP + 200 μM vanadate + 5 mM $MgCl_2$. The primary result of the addition of these reagents would be occupancy of the second NB domain of trapped Pgp with nucleotide. As shown in Figure 5, at 4 °C there was a slight enhancement (~23%) in the intensity of the photolabeled Pgp band when ATP/vanadate/Mg^{2+} were included in the reaction mix. The intensity of photolabeling of the Pgp transition state complex was reduced to 19% relative to untrapped Pgp, and this increased to 36% in the presence of ATP/vanadate/Mg^{2+}. At 22 °C, untrapped Pgp displayed a reduction of labeling intensity to 43% in the presence of ATP/vanadate/Mg^{2+}. Transition state Pgp gave a relative intensity of 42%, and this was reduced to 35% when ATP/vanadate/Mg^{2+} was added. Thus, although there is a reduction in the intensity of azidopine labeling in the transition state, its magnitude depends on both the temperature at which the incubation and cross-linking are carried out and the presence of excess trapping reagents. Since the fluorescence experiments clearly indicated that the transition state binds several drugs with unchanged affinity, the reduction in labeling intensity likely reflects a change in the efficiency of photolabeling of the trapped conformation.

DISCUSSION

Much remains to be learned about the mechanism of Pgp-mediated drug transport. In particular, details of how ATP hydrolysis drives transport, and the point in the catalytic cycle at which drug release takes place, are critical for understanding the mechanism of substrate movement across the lipid bilayer. Vanadate trapping has proved to be a very useful tool in the study of many ATPases, ranging from myosin to ABC transporters, since it allows stabilization of an intermediate in the reaction pathway. The experimental procedure most often followed involves adding ATP, excess vanadate, and a divalent cation (Mg^{2+}, Mn^{2+}, or Co^{2+}) to the ATPase in question. After one catalytic turnover, a complex of ADP·V_i·M^{2+} is tightly bound at the active site; in the case of ABC proteins, only one active site is trapped in this fashion (*30*, *57*, *58*). The vanadate ion likely takes up the position normally occupied by the γ-phosphate of ATP, as observed in the crystal structure of the vanadate-trapped structure of myosin (*59*). When using vanadate trapping as a tool, it is important that at least some experiments be carried out following removal of excess vanadate and other reagents (*27*), since vanadate may bind to other locations within ATPases at high concentrations, as noted for myosin (*60*). In the present study, the more stable Co^{2+}-trapped complex of Pgp was isolated free of excess vanadate by gel filtration chromatography and studied in isolation by both fluorescence quenching experiments and photoaffinity labeling. Because of the shorter lifetime of the Mg^{2+}-trapped complex, excess reagents normally remained in the experimental sample to prevent exit of the protein from the transition state.

There is now substantial evidence that interaction of drug with the substrate binding site of Pgp takes place within the membrane itself. Recent work in our laboratory has mapped the binding site for the fluorescent substrate H33342 to the cytoplasmic side of the membrane bilayer (*21*), in agreement with the concept that the transporter may act as a flippase, moving its substrates from the inner to the outer leaflet (*18*, *22*). Initial binding of drug would clearly be of (relatively) high affinity; however, the affinity must be lowered considerably at some point during the transport cycle to allow drug release from the protein.

Multistep models have been proposed to explain the transport process for Pgp and other ABC family multidrug transporters. An alternating two-site mechanism has been

proposed in the case of LmrA, a bacterial ABC drug efflux pump with considerable functional similarity to Pgp (it can substitute for Pgp in human lung fibroblast cells). The LmrA homodimer is proposed to contain two drug binding sites, either high affinity or low affinity, one within each "half" of the protein (*61*). The ATP-bound form of the protein is associated with high-affinity binding sites facing the cytosol, and the ADP-bound form of the protein is associated with low-affinity binding sites facing the external medium. The vanadate-trapped transition state is thought to possess low-affinity drug binding sites exposed at the extracellular surface. During a single transport cycle, the drug binding sites of LmrA are proposed to alternate from high affinity to low affinity via a conformational change, driven by ATP hydrolysis.

Another multistep model has been proposed by Ambudkar and co-workers for Pgp-mediated drug transport (*62*). In their mechanism, drug initially binds to a single high-affinity site (the "on" site), and later in the catalytic cycle, it is physically moved to a different location within the protein, presumed to be a second drug binding site. The binding affinity of such a site would necessarily be substantially lower (the "off" site), to allow release of the substrate to the external milieu. The energy released during ATP hydrolysis would presumably power the movement of drug from the high-affinity to the low-affinity site. Evidence for such a low-affinity drug binding site was obtained by photoaffinity labeling studies of the vanadate-trapped transition state complex of Pgp, which showed very little binding of the drug IAAP (*34*). The release of ADP from the transition state was also proposed to generate a form of Pgp showing very low drug binding affinity, and it was proposed that a second round of ATP hydrolysis was required to "reset" the transporter and regain high-affinity drug binding (*35*, *63*).

The results of our photolabeling experiments indicate that a reduction in the intensity of labeling with the substrate [^{3}H]azidopine is indeed seen for transition state Pgp. However, this reduction was not large (5-fold maximum) and depended on temperature (it was much smaller at 22 °C compared to 4 °C). In addition, the labeling intensity was also altered in the presence of excess vanadate and ATP. We propose that a reduction in labeling intensity cannot be interpreted as a reduction in binding affinity but rather as a change in the labeling efficiency of Pgp in the transition state, which is known to have a substantially different conformation from the resting state protein (*32*, *33*, *64*). Photolabeling is not an equilibrium method (the labeling efficiency is usually a few percent), and as discussed elsewhere (*65*), it is not suitable for measuring quantitative changes in substrate binding affinity, especially where changes in protein conformation also take place.

In the present work, we have directly measured the binding affinity of the vanadate-trapped transition state complex of purified Pgp using three different fluorescence spectroscopic approaches. The Pgp preparation employed for this study has high ATPase and drug transport activities (*48*, *66*). In addition, we observe close to 100% quenching of the intrinsic Trp fluorescence of the protein by some drugs, such as rhodamine B (*45*), which strongly suggests that virtually all of the protein is functional with respect to drug binding. In the first approach, purified Pgp and the vanadate-trapped complex were labeled with the fluorophore MIANS, and saturable fluorescence quenching was used to estimate the K_d for binding. Using this technique, our laboratory has previously determined the affinity for binding of over 100 different compounds to purified resting state Pgp. The estimated K_d values fall in the range 25 nM to 250 mM (*67*, *68*; P. Lu and F. J. Sharom, unpublished data). In this study, we show that the binding of four MDR substrates and two modulators to both the transition state and the ADP-bound form of Pgp takes place with high affinity. A small decrease in affinity (2-fold) for the MDR drugs tested is likely related to changes in the structure of the transition state, which is known to have an altered conformation, and is clearly insufficient to result in drug release.

In the second approach, we employed native unmodified Pgp and monitored the intrinsic Trp fluorescence of the protein, which we previously showed was quenched in a saturable manner by binding of drug substrates (*45*). Quantitative estimates for K_d values were obtained by fitting of the data to binding curves. Once again, we saw very little difference in the binding affinity of vinblastine and doxorubicin to the transition state or the ADP-bound state, relative to the resting state protein.

Finally, we used the fluorescent dye H33342, a high-affinity substrate for Pgp whose fluorescence emission is greatly enhanced upon binding to the unmodified protein (*21*). Fitting of the fluorescence enhancement data to binding curves clearly showed that the affinity of H33342 for transition state and resting Pgp was identical. The metal ion used to form the transition state is also of no consequence, except that it alters the stability of the resulting complex. We obtained identical results using both Co^{2+} and Mg^{2+} ions in different experiments.

The experimental data suggest that drug has already been lost from the transporter, presumably as a direct result of the transport process, before the formation of the vanadate-trapped transition state. If it is assumed that substrate dissociation during the transport cycle must result from a large decrease in drug binding affinity, then it is clear that Pgp has already reattained its high-affinity drug binding characteristics at the transition state stage. Our results are in agreement with the proposal of a concerted transport mechanism put forward by Davidson and co-workers for the bacterial maltose permease, $MalFGK_2$. The maltose substrate is delivered to the membrane-bound MalFG complex by the periplasmic maltose binding protein, MalE, which remains tightly bound to the vanadate-trapped transition state complex (*58*). They demonstrated that maltose transport was already complete prior to formation of the vanadate-trapped complex. The maltose permease transition state did not appear to be contain bound maltose, suggesting that it has low substrate binding affinity. However, this ABC protein differs from Pgp in several ways. First, the bacterial periplasmic binding protein-dependent transporters are the only members of the ABC superfamily to use an accessory protein to bind the substrate. Second, the vanadate-trapped complex cannot be formed from ADP but only from ATP after one round of hydrolysis (*57*). In contrast, Pgp readily forms a vanadate-trapped complex from both ATP and ADP (*30*). Thus it is possible that the Pgp vanadate-trapped transition state is farther along the reaction pathway than that of the maltose permease, so that it has regained its high-affinity state via conformational relaxation. It should also be kept in mind

that the vanadate-trapped complex is only a "surrogate" for the native transition state, which is presumably very short-lived. Another possibility for consideration is that drug release could occur at a later stage in the catalytic cycle, for example, following dissociation of ADP. However, we show in the present work that the ADP-bound form of Pgp also binds drugs with unchanged affinity, making this possibility unlikely.

Thus the results of the present study suggest a mechanism involving concerted conformational changes, rather than a multistep mechanism, for transport of drugs by Pgp. A recent FTIR study (*64*) used ^{2}H exchange to demonstrate that ATP hydrolysis drives conformational changes in Pgp which affect its accessibility to the external medium. In particular, the vanadate-trapped transition state showed a large increase in the exchange rate, although the overall secondary structure was not significantly altered. The free energy released by ATP hydrolysis must generate a high-energy intermediate during catalysis, as proposed by Senior and co-workers (*31*). The relaxation of this intermediate would drive simultaneous movement of drug across the membrane, which is apparently completed prior to formation of the vanadate-trapped complex. The fact that the transition state complex binds drugs with normal high affinity indicates that switching of the drug binding site from high affinity to low affinity and back to high affinity has already taken place at this stage of the transport cycle.

REFERENCES

1. Dassa, E., and Bouige, P. (2001) *Res. Microbiol. 152*, 211−229.
2. Higgins, C. F. (2001) *Res. Microbiol. 152*, 205−210.
3. Dean, M., and Allikmets, R. (2001) *J. Bioenerg. Biomembr. 33*, 475−479.
4. Sánchez-Fernández, R., Davies, T. G. E., Coleman, J. O. D., and Rea, P. A. (2001) *J. Biol. Chem. 276*, 30231−30244.
5. Saurin, W., Hofnung, M., and Dassa, E. (1999) *J. Mol. Evol. 48*, 22−41.
6. Holland, I. B., and Blight, M. A. (1999) *J. Mol. Biol. 293*, 381−399.
7. Schneider, E., and Hunke, S. (1998) *FEMS Microbiol. Rev. 22*, 1−20.
8. Linton, K. J., and Higgins, C. F. (1998) *Mol. Microbiol. 28*, 5−13.
9. Putman, M., Van Veen, H. W., and Konings, W. N. (2000) *Microbiol. Mol. Biol. Rev. 64*, 672−693.
10. Putman, M., Van Veen, H. W., Degener, J. E., and Konings, W. N. (2000) *Mol. Microbiol. 36*, 772−773.
11. Wolfger, H., Mamnun, Y. M., and Kuchler, K. (2001) *Res. Microbiol. 152*, 375−389.
12. Litman, T., Druley, T. E., Stein, W. D., and Bates, S. E. (2001) *Cell. Mol. Life Sci. 58*, 931−959.
13. Bates, S. E., Robey, R., Miyake, K., Rao, K., Ross, D. D., and Litman, T. (2001) *J. Bioenerg. Biomembr. 33*, 503−511.
14. Gottesman, M. M. (2002) *Annu. Rev. Med. 53*, 615−627.
15. Gottesman, M. M., and Ambudkar, S. V. (2001) *J. Bioenerg. Biomembr. 33*, 453−458.
16. Sharom, F. J. (1997) *J. Membr. Biol. 160*, 161−175.
17. Ambudkar, S. V., Dey, S., Hrycyna, C. A., Ramachandra, M., Pastan, I., and Gottesman, M. M. (1999) *Annu. Rev. Pharmacol. Toxicol. 39*, 361−398.
18. Higgins, C. F., and Gottesman, M. M. (1992) *Trends Biochem. Sci. 17*, 18−21.
19. Romsicki, Y., and Sharom, F. J. (1999) *Biochemistry 38*, 6887−6896.
20. Lu, P., Liu, R., and Sharom, F. J. (2001) *Eur. J. Biochem. 268*, 1687−1697.
21. Qu, Q., and Sharom, F. J. (2002) *Biochemistry 41*, 4744−4752.
22. Romsicki, Y., and Sharom, F. J. (2001) *Biochemistry 40*, 6937−6947.
23. Chang, G., and Roth, C. B. (2001) *Science 293*, 1793−1800.
24. Locher, K. P., Lee, A. T., and Rees, D. C. (2002) *Science 296*, 1091−1098.
25. Jones, P. M., and George, A. M. (1999) *FEMS Microbiol. Lett. 179*, 187−202.
26. Hopfner, K. P., Karcher, A., Shin, D. S., Craig, L., Arthur, L. M., Carney, J. P., and Tainer, J. A. (2000) *Cell 101*, 789−800.
27. Fetsch, E. E., and Davidson, A. L. (2002) *Proc. Natl. Acad. Sci. U.S.A. 99*, 9685−9690.
28. Qu, Q., and Sharom, F. J. (2001) *Biochemistry 40*, 1413−1422.
29. Urbatsch, I. L., Gimi, K., Wilke-Mounts, S., Lerner-Marmarosh, N., Rousseau, M. E., Gros, P., and Senior, A. E. (2001) *J. Biol. Chem. 276*, 26980−26987.
30. Urbatsch, I. L., Sankaran, B., Weber, J., and Senior, A. E. (1995) *J. Biol. Chem. 270*, 19383−19390.
31. Senior, A. E., al-Shawi, M. K., and Urbatsch, I. L. (1995) *FEBS Lett. 377*, 285−289.
32. Julien, M., and Gros, P. (2000) *Biochemistry 39*, 4559−4568.
33. Rosenberg, M. F., Velarde, G., Ford, R. C., Martin, C., Berridge, G., Kerr, I. D., Callaghan, R., Schmidlin, A., Wooding, C., Linton, K. J., and Higgins, C. F. (2001) *EMBO J. 20*, 5615−5625.
34. Ramachandra, M., Ambudkar, S. V., Chen, D., Hrycyna, C. A., Dey, S., Gottesman, M. M., and Pastan, I. (1998) *Biochemistry 37*, 5010−5019.
35. Sauna, Z. E., and Ambudkar, S. V. (2000) *Proc. Natl. Acad. Sci. U.S.A. 97*, 2515−2520.
36. Wang, G., Pincheira, R., and Zhang, J. T. (1998) *Eur. J. Biochem. 255*, 383−390.
37. Peterson, G. L. (1977) *Anal. Biochem. 83*, 346−356.
38. Doige, C. A., Yu, X., and Sharom, F. J. (1992) *Biochim. Biophys. Acta 1109*, 149−160.
39. Sharom, F. J., Yu, X., Chu, J. W. K., and Doige, C. A. (1995) *Biochem. J. 308*, 381−390.
40. Liu, R., and Sharom, F. J. (1996) *Biochemistry 35*, 11865−11873.
41. Mayer, L. D., Bally, M. B., Hope, M. J., and Cullis, P. R. (1985) *Biochim. Biophys. Acta 816*, 294−302.
42. Mayer, L. D., Hope, M. J., and Cullis, P. R. (1986) *Biochim. Biophys. Acta 858*, 161−168.
43. Lakowicz, J. R. (1999) in *Principles of Fluorescence Spectroscopy*, 2nd ed., Kluwer Academic Publishers, New York.
44. Parker, C. A. (1968) in *Photoluminescence of Solutions*, Elsevier Publishing Co., Amsterdam.
45. Liu, R., Siemiarczuk, A., and Sharom, F. J. (2000) *Biochemistry 39*, 14927−14938.
46. Loe, D. W., and Sharom, F. J. (1994) *Biochim. Biophys. Acta 1190*, 72−84.
47. Loo, T. W., and Clarke, D. M. (1995) *J. Biol. Chem. 270*, 22957−22961.
48. Liu, R., and Sharom, F. J. (1997) *Biochemistry 36*, 2836−2843.
49. Sharom, F. J., Lu, P., Liu, R., and Yu, X. (1998) *Biochem. J. 333*, 621−630.
50. Martin, C., Higgins, C. F., and Callaghan, R. (2001) *Biochemistry 40*, 15733−15742.
51. Druley, T. E., Stein, W. D., and Roninson, I. B. (2001) *Biochemistry 40*, 4312−4322.
52. Doppenschmitt, S., Langguth, P., Regardh, C. G., Andersson, T. B., Hilgendorf, C., and Spahn-Langguth, H. (1999) *J. Pharmacol. Exp. Ther. 288*, 348−357.
53. Shapiro, A. B., and Ling, V. (1997) *Eur. J. Biochem. 250*, 122−129.
54. Shapiro, A. B., Corder, A. B., and Ling, V. (1997) *Eur. J. Biochem. 250*, 115−121.
55. Sharom, F. J., DiDiodato, G., Yu, X., and Ashbourne, K. J. (1995) *J. Biol. Chem. 270*, 10334−10341.
56. Sharom, F. J., Yu, X., DiDiodato, G., and Chu, J. W. K. (1996) *Biochem. J. 320*, 421−428.
57. Sharma, S., and Davidson, A. L. (2000) *J. Bacteriol. 182*, 6570−6576.
58. Chen, J., Sharma, S., Quiocho, F. A., and Davidson, A. L. (2001) *Proc. Natl. Acad. Sci. U.S.A. 98*, 1525−1530.
59. Smith, C. A., and Rayment, I. (1996) *Biochemistry 35*, 5404−5417.
60. Cremo, C. R., Long, G. T., and Grammer, J. C. (1990) *Biochemistry 29*, 7982−7990.
61. Van Veen, H. W., Margolles, A., Müller, M., Higgins, C. F., and Konings, W. N. (2000) *EMBO J. 19*, 2503−2514.
62. Sauna, Z. E., Smith, M. M., Müller, M., Kerr, K. M., and Ambudkar, S. V. (2001) *J. Bioenerg. Biomembr. 33*, 481−491.
63. Sauna, Z. E., and Ambudkar, S. V. (2001) *J. Biol. Chem. 276*, 11653−11661.

64. Vigano, C., Julien, M., Carrier, I., Gros, P., and Ruysschaert, J. M. (2002) *J. Biol. Chem. 277*, 5008−5016.
65. Qu, Q., Russell, P. L., and Sharom, F. J. (2003) *Biochemistry* (in press).
66. Sharom, F. J., Yu, X., and Doige, C. A. (1993) *J. Biol. Chem. 268*, 24197−24202.
67. Sharom, F. J., Liu, R., Qu, Q., and Romsicki, Y. (2001) *Semin. Cell Dev. Biol. 12*, 257−266.
68. Sharom, F. J., Liu, R., Romsicki, Y., and Lu, P. (1999) *Biochim. Biophys. Acta 1461*, 327−345.

BI0267745